


 Cite this: *RSC Adv.*, 2020, 10, 18477

# Compatibilization of porphyrins for use as high permittivity fillers in low voltage actuating silicone dielectric elastomers†

 Cody B. Gale,<sup>a</sup> Michael A. Brook<sup>\*a</sup> and Anne Ladegaard Skov<sup>\*b</sup>

Polysiloxanes represent, because of their unusual properties, a material with great potential for use in dielectric elastomers (DEs), a promising class of electroactive polymers. Currently, their application as actuators is limited by the need for high driving voltages, as a result of the low relative permittivity possessed by polysiloxanes (~2–3). Reducing these voltages can be achieved to some degree by using high permittivity additives to improve the permittivity of the polysiloxane. However, modifying such additives so that they are compatible with, and can be dispersed within, polysiloxane elastomers remains challenging. For reliable actuation, full miscibility is key. In this work the porphyrin 5,10,15,20-(tetra-3-methoxyphenyl)porphyrin (TPMP) was investigated as a high permittivity additive. Its behaviour was compared to the analogue that was derivatized with bis(trimethylsiloxy)methylsilane groups using the Piers–Rubinsztajn reaction to improve compatibility with silicone formulations. The derivatized porphyrin was dispersed in elastomers and their dielectric and mechanical properties were evaluated. It was discovered that only low levels of incorporation (1–10%) of the siliconized TPMP – much lower than the parent TPMP – were needed to elicit improvements in the permittivity and electromechanical actuation of the elastomers; actuation strains of up to 43% could be achieved using this method.

 Received 27th February 2020  
 Accepted 7th May 2020

DOI: 10.1039/d0ra01872d

[rsc.li/rsc-advances](http://rsc.li/rsc-advances)

## Introduction

Dielectric elastomers (DEs), commonly referred to as “artificial muscles”, are a class of electroactive polymers receiving considerable attention for their potential applications in soft robotics and clean energy applications.<sup>1,2</sup> They consist of two components; a thin incompressible elastomer, and two compliant electrodes that are assembled such that the elastomer is sandwiched between the compliant electrodes that are connected to an external voltage source.<sup>3</sup> When a voltage is applied, charge builds up on the electrodes exerting a pressure on the elastomer. The actuation of the elastomer is spontaneous, as it serves to reduce the charge density present on the electrodes while simultaneously bringing the oppositely charged electrodes into proximity to one another.<sup>4</sup>

Three parameters govern the electromechanical response or strain exhibited by DEs; the relative permittivity ( $\epsilon_r$ ) or susceptibility of elastomer to polarization; Young’s modulus ( $Y$ ); and

dielectric breakdown strength ( $E_b$ ), which is the maximum voltage that can be applied to the elastomer before it short circuits. The actuation can be described by eqn (1),

$$s = \frac{\epsilon_0 \epsilon_r}{Y} \left( \frac{V}{d} \right)^2 \quad (1)$$

and the ideal elastomer is one that exhibits a high relative permittivity and dielectric breakdown strength while simultaneously having a low Young’s modulus.<sup>1,5</sup> Given the potential of DEs as artificial muscles, there has been widespread investigation into materials that possess optimal properties.

While a variety of elastomeric materials have been investigated, polysiloxanes have come to be considered the premier material for dielectric applications due to their excellent mechanical and physicochemical properties. Specifically, polysiloxanes show minimal aging effects, reproducible actuation for millions of cycles, high thermal stability and lower viscous losses than their competitors.<sup>1</sup> Unfortunately, polysiloxanes suffer from one critical flaw; low relative dielectric permittivities (~2–3), which results in the need for higher driving voltages to achieve actuation strains comparable to other materials such as VHB from 3M. As a consequence, there is significant interest in developing strategies to increase the permittivity of polysiloxanes.<sup>1,4,6</sup>

Of the multiple strategies investigated to improve the permittivity of polysiloxanes, including conductive fillers, and the grafting of permanent dipoles, the most prevalent strategy

<sup>a</sup>Department of Chemistry and Chemical Biology, McMaster University, 1280 Main St., W., Hamilton, ON, L8S 4M1, Canada. E-mail: mabrook@mcmaster.ca

<sup>b</sup>Department of Chemical and Biochemical Engineering, Technical University of Denmark, Søtofts Plad 227s, Kgs. Lyngby, DK-2800, Denmark. E-mail: al@kt.dtu.dk

† Electronic supplementary information (ESI) available: <sup>1</sup>H, <sup>13</sup>C and <sup>29</sup>Si NMR data of TPMP-Bis-H, figures showing relative permittivity, dielectric loss, tan( $\delta$ ) and tables giving electrical breakdown strength of Zn-TPMP and Zn-TPMP-Bis-H in homemade and commercial elastomers. See DOI: 10.1039/d0ra01872d



involves the doping of elastomers with high permittivity inorganic additives. This strategy has received attention due to its simplicity; control over the permittivity can be realized simply by adding dopants into commercially available silicone elastomer formulations.<sup>7,8</sup> Additives such as TiO<sub>2</sub>,<sup>9–11</sup> ZnO,<sup>12</sup> and BaTiO<sub>3</sub><sup>13,14</sup> have all been tested as high permittivity fillers. In each case, these fillers have resulted in improved permittivities the magnitude of which depends on the loading of the additive. The increase in the dielectric permittivity of the elastomers was usually maximum of the order of 2. Unfortunately, this strategy is not without its challenges. Achieving reproducible dispersions and minimizing particle aggregation is difficult, and aggregates significantly and negatively impact the final dielectric properties of the composite.<sup>15</sup> In addition, inorganic additives act as fillers that increase the  $\gamma$  of the materials, ultimately resulting in materials with poorer actuation performance since the Young's modulus was usually increased by more than a factor of 2.<sup>16</sup>

Electro-stabilization by means of inorganic fillers, such as ZnO and BaTiO<sub>3</sub>, has also been explored<sup>17,18</sup> but again the favourable dielectric properties achieved are outweighed by the increased Young's modulus.<sup>12,19</sup>

While inorganic fillers such as those discussed above have been widely investigated, organic fillers have received considerably less attention. The investigation into organic fillers has largely been limited to conjugated polymers with limited miscibility with silicone, such as polyaniline, and poly(hexylthiophene), which all serve to increase the dielectric performance but only to a limited extent: increasing the concentration of the dopant within the elastomer is challenging due to the immiscibility of the two components.<sup>20,21</sup> Phase separation leads to unfavourable properties due to the resulting inhomogeneous electrical fields. An excellent example of the use of a high-permittivity organic filler in DE applications was conducted by Zhang *et al.* Using copper-phthalocyanine oligomers (CPO), they were able to increase the permittivity of silicone elastomers to ~11 at a loading of 40%, which represents a 250% increase in the permittivity.<sup>22,23</sup> Macrocycles such as phthalocyanines have a tendency to form aggregates, particularly in silicones due to their low solubility.<sup>24,25</sup> Zhang *et al.* observed aggregation of the CPO in their elastomers, which contributed to a significant lowering of the dielectric breakdown strength.<sup>22</sup>

Despite the promise shown by these organic fillers there has been little additional investigation into the use of these or other high permittivity fillers aromatic macrocycles, such as porphyrins (a closely related class of molecules to phthalocyanines) for silicone elastomers. We reasoned that the benefits of this class of molecules could be better realized if the materials were more soluble in silicones.

It has been shown that highly insoluble triarylamines could be rendered soluble in silicones by grafting small silicone units onto the aromatic ring. The Piers–Rubinsztajn (PR) reaction was used to convert arylmethoxy into arylsiloxy groups, analogous to the reaction shown in Fig. 1B, after which they became soluble in a variety of non-polar solvents.<sup>26–28</sup> We hypothesized that the same reaction could

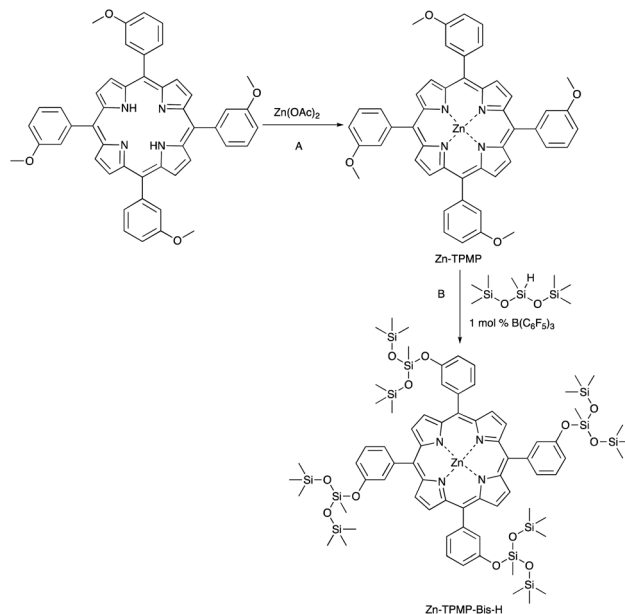


Fig. 1 (A) Synthesis of Zn-TPMP. (B) Synthesis of Zn-TPMP-Bis-H.

be used with an appropriate porphyrin and silane to create liquid porphyrins that, due to their silicone functionality, would similarly show improved dispersion in silicone elastomers. In this work, 5,10,15,20-(tetra-3-methoxyphenyl)porphyrin (TPMP) was derivatized with bis(trimethylsiloxy)methylsilane and the resulting silicone-modified porphyrin was incorporated into silicone elastomer formulations at various loadings. The physical and dielectric properties of the elastomers were evaluated and compared to elastomers containing unmodified TPMP. A comparison with unmodified silicone elastomers was also performed.

## Experimental

### Materials

5,10,15,20-(Tetra-3-methoxyphenyl)porphyrin (TPMP) was purchased from Porphychem, France. Zinc acetate dihydrate, tris-(triphenylphosphine)rhodium(i) chloride (Wilkinson's Catalyst), neutral alumina Brockmann I activity, dichloromethane, methanol, *n*-pentane and deuterated chloroform were purchased from Sigma-Aldrich. Wilkinson's catalyst was dissolved in toluene to provide a stock solution of 7.6 mg mL<sup>-1</sup> (76 mg in 10 mL). Bis(trimethylsiloxy)methylsilane, trimethylsiloxy-terminated dimethylsiloxane-hydromethyl-siloxane copolymer (25–35% hydromethylsiloxane, HMS-301,  $M_w = 1900\text{--}2000\text{ g mol}^{-1}$ , 25–35 cSt), and vinyl-terminated polydimethylsiloxane (DMS-V22,  $M_w = 9400\text{ g mol}^{-1}$ , 200 cSt) were purchased from Gelest. Elastosil RT 625 Parts A and B were purchased from Wacker Chemie. Tris-(pentafluorophenyl)borane (B(C<sub>6</sub>F<sub>5</sub>)<sub>3</sub>, BCF) was purchased from TCI chemicals and dissolved in dichloromethane to provide a stock solution of 10 mg mL<sup>-1</sup>. Karstedt's catalyst, platinum divinyl-tetramethyl disiloxane complex, was purchased from ABCR chemicals. All chemicals were used as received without further purification. Carbon Grease (Nyogel 756G, Lot# MY121102) was



purchased from Nye Lubricants Inc. The Dual Asymmetric Centrifuge (DAC) Model DAC 150.1 FV7-K and FlackTek cups were purchased from FlackTek Incorporated.

### NMR analysis

$^1\text{H}$ ,  $^{13}\text{C}$  NMR and  $^{29}\text{Si}$  NMR spectra were performed on a Bruker Avance 600 MHz NMR.  $\text{CDCl}_3$  was used as the solvent in each case.

### Infrared spectroscopy

Fourier transform infrared spectroscopy was performed using a Nicolet is50 FT-IR instrument.

### Electrospray ionization mass spectrometry

Electrospray ionization mass spectrometry (ESI-MS) was performed using an Agilent 6340 Ion Trap mass spectrometer. Sample concentrations were  $\sim 50$ – $100\ \mu\text{M}$ .

### Dielectric spectroscopy

Dielectric spectroscopy was performed using a Novocontrol Alpha-A High Performance Frequency Analyzer (Novo-control Technologies GmbH & Co. KG, Germany). Measurements were taken in the frequency range of  $10^{-1}$  to  $10^{-6}$  Hz at  $25^\circ\text{C}$ . Samples were sandwiched between two gold-coated electrode plates prior to measurement. The electrode geometry was 20 mm.

### Dielectric breakdown

Electrical breakdown strength was measured using an in-house-built device based on international standards (IEC 60243-1 (1998) and IEC 60243-2 (2001)). Samples were prepared with a thickness of 100  $\mu\text{m}$ . The film was placed between two spherical electrodes (diameter of 20 mm). The electrical breakdown measurement was taken at the point of contact with a stepwise increasing voltage applied (50–100 V per step) at a rate of 0.5–1 steps per s. The electrical breakdown measurement was repeated 12 times for each sample, and the average of these values was then stated as the electrical breakdown strength.

### Young's modulus

Young's moduli were measured using an Instron 3345 instrument. Samples were prepared as thin films of  $\sim 200\ \mu\text{m}$  and were stretched at a rate of  $500\ \text{mm}\ \text{min}^{-1}$ . The Young's moduli were calculated by taking the tangent of the stress-strain curve at 10% strain. Each sample was subject to three trials.

### Synthesis of zinc 5,10,15,20-(tetra-3-methoxyphenyl)porphyrin (Zn-TPMP)

TPMP (5.00 g, 6.80 mmol) was added to a 2 L round-bottomed flask and dissolved in 1 L of a DCM:methanol mixture (1 : 1). Zinc acetate dihydrate (2.98 g, 14.0 mmol) was added, and the reaction mixture was stirred vigorously for 5 h. The solvent was removed *in vacuo* to yield a purple solid that was suspended in methanol and collected *via* vacuum filtration. The product was

rinsed with water ( $3 \times 100\ \text{mL}$ ) to remove excess zinc acetate and dried overnight to yield a purple solid (5.15, 6.45 mmol, 95%).

$^1\text{H}$  NMR (600 MHz,  $\text{CDCl}_3$ )  $\delta$  8.99 (s, 8H), 7.83–7.77 (m), 7.63 (t,  $J = 7.9\ \text{Hz}$ , 4H), 7.31 (dd,  $J = 8.6, 2.5\ \text{Hz}$ , 4H), 3.95 (s, 12H).  $^{13}\text{C}$  NMR (151 MHz,  $\text{CDCl}_3$ )  $\delta$  157.77, 150.13, 144.11, 132.00, 127.60, 127.31, 120.87, 120.34, 113.44, 55.48. MS-ESI: calc. for  $\text{C}_{48}\text{H}_{36}\text{N}_4\text{O}_4\text{Zn}$ , 796.2028; found, 796.2026.

### Synthesis of Zn-TPMP-Bis-H

Zn-TPMP (5.00 g, 6.26 mmol) and bis(trimethylsiloxy)methylsilane (11.1 g, 50.1 mmol, 14.0 mL) were added to a 1 L round-bottomed flask and dissolved in 250 mL of DCM. Tris(pentafluorophenyl)borane solution (14.0 mL, 255 mg, 0.498 mmol, 1 mol%) was added. The reaction was monitored *via* thin-layer chromatography using a 1 : 1 *n*-pentane : DCM mixture, the reaction was judged complete when all the Zn-TPMP was consumed ( $\sim 3\ \text{h}$ ). The solvent was removed *in vacuo* and the product was purified using column chromatography on Brockman Neutral Alumina Activity I with 1 : 1 pentane : DCM to yield a purple liquid (9.27 g, 5.71 mmol, 91.2%).  $^1\text{H}$  NMR (600 MHz,  $\text{CDCl}_3$ )  $\delta$  9.16 (s, 8H), 8.09–7.89 (m, 8H), 7.84–7.67 (m, 4H), 7.57–7.42 (m, 4H), 0.46 (s, 12H), 0.25 (q,  $J = 1.3\ \text{Hz}$ , 72H).  $^{13}\text{C}$  NMR (151 MHz,  $\text{CDCl}_3$ )  $\delta$  152.54, 150.18, 144.21, 132.03, 128.50, 127.26, 126.52, 120.76, 119.12, 1.74,  $-3.02$ .  $^{29}\text{Si}$  NMR (119 MHz,  $\text{CDCl}_3$ )  $\delta$  9.82,  $-60.09$ . Calc. for  $\text{C}_{72}\text{H}_{108}\text{N}_4\text{O}_{12}\text{Si}_{12}\text{Zn}$  1623.4528; found 1623.4533.

### Preparation of stock hydrosilylation pre-elastomer (without platinum catalyst)

HMS-301 (3.13 g, 1.56 mmol, 12.76 mmol Si-H) and DMS-V22 (60.00 g, 6.38 mmol, 12.76 mmol vinyl) were added to a 60 mL FlackTek cup (Si-H : vinyl = 1 : 1) and mixed at 3500 rpm for five minutes to ensure a homogenous mixture. Silicone pre-elastomers were subject to high vacuum treatment after mixing, but prior to cure to reduce bubble formation in the elastomers.

### Preparation of porphyrin elastomers-physical dispersion of Zn-TPMP and Zn-TPMP-Bis-H in stock pre-elastomer

The appropriate amount of the stock pre-elastomer and Zn-TPMP or Zn-TPMP-Bis-H (Table 1) were added to a 25 mL

Table 1 Required masses for porphyrin elastomers using HMS-301+DMS-V22 mixture

Weight percent, porphyrin (%)	Mass, Zn-TPMP or Zn-TPMP-Bis-H (g)	Mass, silicone mixture (g)	Total mass (g)
0	0	1.500	1.50
0.5	0.00750	1.493	1.50
1	0.0150	1.485	1.50
2	0.0300	1.470	1.50
4	0.0600	1.440	1.50
6	0.0900	1.410	1.50
8	0.120	1.380	1.50
10	0.150	1.350	1.50



Table 2 Required masses for the synthesis of porphyrin elastomers using Elastosil 625

Weight percent, porphyrin (%)	Total mass (g)	Mass, Zn-TPMP-Bis-H (g)	Mass silicone (g)	Mass RT 625 Part A (g)	Mass RT 625 Part B (g)
0	1.500	0	1.500	1.350	0.150
2	1.500	0.0300	1.470	1.323	0.147
6	1.500	0.0900	1.410	1.269	0.141
10	1.500	0.150	1.350	1.215	0.135

FlackTek cup and mixed at 3500 rpm for 2 min in the DAC to disperse the respective porphyrin additives. Karstedt's catalyst (0.5  $\mu\text{L}$ , 6 ppm) was added and then mixed at 1500 rpm for 30 s. The mixture was poured into 1 mm square molds and cured at 80  $^{\circ}\text{C}$  for 5 h, providing an elastomer  $\sim$ 1 mm thick to measure dielectric properties.

### Preparation of porphyrin elastomers-physical dispersion of Zn-TPMP-Bis-H in Elastosil 625

The appropriate amount of Zn-TPMP-Bis-H and Elastosil 625 Parts A and B (Table 2) were added to a 25 mL FlackTek cup and mixed at 3500 rpm for 2 min. Additional Karstedt's catalyst (0.5  $\mu\text{L}$ , 6 ppm) or Wilkinson's catalyst (1.2  $\mu\text{L}$ , 6 ppm) was added to each elastomer to ensure consistency, and the formulation was mixed for an additional 1 min at 2500 rpm. The final cross-linked films were prepared in three thicknesses: 1 mm to measure LVE and dielectric properties, 100  $\mu\text{m}$  to measure dielectric breakdown strength, and 200  $\mu\text{m}$  to measure Young's modulus. Each sample was cured at 80  $^{\circ}\text{C}$  for 5 h.

### Actuation tests

Elastomers containing 0, 2, 6 and 10% Zn-TPMP-Bis-H were made using the procedure described above and cast as 50  $\mu\text{m}$  films. The films were stretched over a rigid ring mold (inner diameter = 5 cm, outer diameter = 7 cm) such that a 10% pre-strain was applied. A 25 mm diameter circular carbon grease electrode was applied to each side and connected to a Stanford Research Systems Model PS37 high voltage source. An initial voltage of 100 V was applied, and the voltage was gradually increased in 50 V increments until dielectric breakdown was observed. The change in diameter of the electrode was measured by analyzing the videos with the software tracker and this data was used to calculate the % area strain.

## Results and discussion

### Synthesis of Zn-TPMP and Zn-TPMP-Bis-H

The addition of zinc to the parent TPMP porphyrin to give Zn-TPMP (Fig. 1A) was readily achieved at room temperature in high yields (95%); metalation of the porphyrin was confirmed after 5 h by monitoring the  $^1\text{H-NMR}$  spectrum for the absence of a peak at  $-2$  ppm in the  $^1\text{H-NMR}$ , corresponding to N-H protons of the pyrrole units.<sup>29</sup> The final product required minimal purification; rinsing the product with water provided a product of sufficient purity for synthesis of Zn-TPMP-Bis-H (Fig. 1B). The metalation of TPMP was determined to be

a necessary step in the synthesis of silylated TPMP, as previous attempts to directly react TPMP *via* the PR reaction were unsuccessful. With the metalated porphyrin, by contrast, the synthesis of the silylated derivative, Zn-TPMP-Bis-H, could be achieved readily at room temperature in a yield of 91% provided sufficient  $\text{B}(\text{C}_6\text{F}_5)_3$  catalyst ( $\sim$ 1 mol%) was used. Concentrations below this value resulted in no reaction even under reflux in toluene. Unlike the starting material, which is a solid, Zn-TPMP-Bis-H is a liquid at room temperature and is soluble in a wide array of polar and non-polar solvents including hexanes, pentane, toluene, and dichloromethane.

### Preparation of elastomers: physical dispersion of porphyrins

**Zn-TPMP.** Elastomers were synthesized using a platinum cure system composed of HMS-301 (multifunctional hydride PDMS crosslinker) and DMS-V22 (telechelic vinyl functional PDMS). This system was selected to evaluate the potential of Zn-TPMP as a dielectric filler without the additives and fillers commonly found in commercial formulations. Initially, Zn-TPMP was physically dispersed in various weight percentages into the formulation and cured into elastomers  $\sim$ 1 mm thick. This technique resulted in elastomers with inhomogeneous dispersions of porphyrin. While samples containing 2–10% initially appeared to be homogenous (Fig. 2A), agglomeration of porphyrin could be readily observed in the 10% sample when observed under an optical microscope (Fig. 2B) or by eye in the

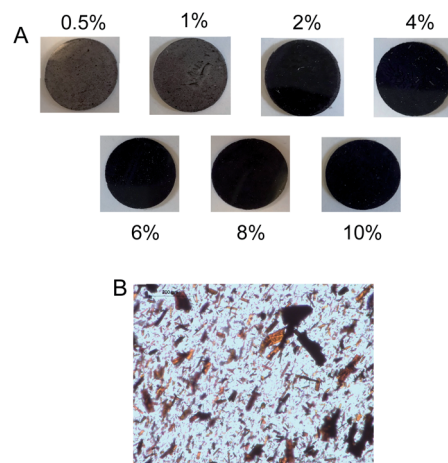


Fig. 2 (A) Elastomers with increasing weight percentages of Zn-TPMP, 1 mm thick. (B) Optical microscope image of a 10% Zn-TPMP elastomer, 100  $\mu\text{m}$  thick.

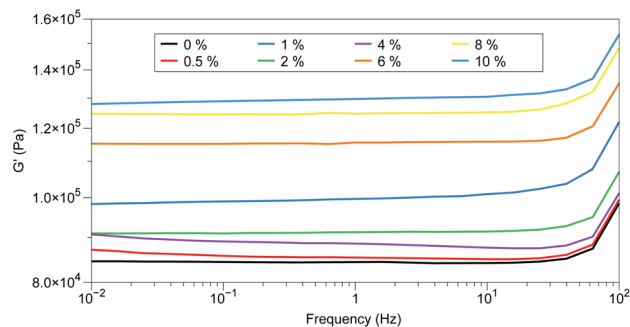


**Table 3** Summary of dielectric properties and shore OO hardness of elastomers with varying weight percentages of Zn-TPMP

Weight%, Zn-TPMP	Permittivity @ 0.1 Hz	$\tan \delta$ @ 0.1 Hz	Conductivity @ 0.1 Hz	Shore OO
0	3.08	0.018	$1.16 \times 10^{-13}$	65
0.5	3.08	0.042	$1.16 \times 10^{-13}$	65
1	3.03	0.086	$1.14 \times 10^{-13}$	65
2	3.1	0.046	$1.17 \times 10^{-13}$	66
4	2.99	0.031	$1.11 \times 10^{-13}$	66
6	3.03	0.042	$1.22 \times 10^{-13}$	66
8	3.03	0.050	$1.13 \times 10^{-13}$	67
10	3.18	0.046	$1.21 \times 10^{-13}$	69

samples containing 0.5–1% porphyrin, as the low concentrations of porphyrin in these cases produced transparent elastomers in which agglomeration could be observed.

Attempts to improve the dispersions by increasing the mixing time or speed ultimately proved unsuccessful, as did pre-dissolving the porphyrin in DCM prior to dispersal. The latter technique resulted in elastomers with defects (voids) due to evaporation of the solvent during the curing process. When evaluated for their dielectric properties, little deviation from the control could be observed, the measured relative permittivities are all within the range generally accepted for unmodified silicone elastomers (2.5–3) and are similar to that of the permittivity measured for the control.<sup>1</sup> Additionally, the conductivity of the elastomers remained unchanged regardless of the amount of additive used. However, while the relative dielectric loss ( $\tan \delta$ ) of the Zn-TPMP samples were similar, they were all slightly lower than the control (Table 3). The poor performance of Zn-TPMP as a dielectric filler is not surprising, as it well known that the potential of a dielectric filler is directly related to its miscibility in the silicone elastomer, with the highest performance achieved with fillers that are fully miscible in the elastomer formulation.<sup>30</sup> Mechanical characterization of these elastomers was hindered by the tendency of the PDMS system to tear during handling, a common problem for silicone elastomers that don't contain reinforcing agents.<sup>31</sup> As a consequence, mechanical characterization could not be performed to determine the Young's moduli of the materials. In place of Young's moduli, the Shore OO hardnesses, a measurement of a materials resistance to indentation, were measured to determine the impact of Zn-TPMP on the mechanical properties of the elastomers. It was observed that at the highest loadings, 8 and 10%, the Shore OO hardness increased while, at lower loadings 0.5–6%, the Shore OO hardness was only one unit higher than the control (Table 3). Given the sensitivity of the Shore OO durometer, these values can all be considered equal within error. Analysis of the storage moduli of the materials confirmed that increasing the loading of Zn-TPMP resulted in harder materials with the storage moduli increasing as the loading of Zn-TPMP increased. While the effect of Zn-TPMP at low loadings is minimal, and within the accepted error window of 10% for rheological data, at higher loadings (6–10%), the effect on storage modulus can be clearly observed. In this case it is

**Fig. 3** Storage modulus ( $G'$ ) of Zn-TPMP homemade elastomers @ 25 °C.

believed that at higher loadings the Zn-TPMP is acting as a very weak reinforcing agent (Fig. 3).

**Zn-TPMP-Bis-H.** The same procedure as described for Zn-TPMP was adapted for the synthesis of elastomers containing Zn-TPMP-Bis-H. Unlike Zn-TPMP, Zn-TPMP-Bis-H readily dispersed in the HMS-301+DMS-V22 pre-elastomer mixture because, it is inferred, the bis(trimethylsiloxy) groups on the porphyrin help to facilitate its incorporation into the pre-elastomer mixture. Once dispersed, homogenous elastomers were produced at loadings of 0.5–4%; at loadings above this phase separation of the Zn-TPMP-Bis-H could be seen in the optical micrographs, presenting as dark regions (Fig. 4). This suggests that 4% is the upper loading limit that can be achieved before the porphyrin oil begins to phase separate from the elastomer mixture.

In the extreme cases of the 8 and 10% porphyrin-containing elastomers, purple Zn-TPMP-Bis-H would readily transfer to filter paper from the elastomer if a force greater than gravity (e.g., a weight) was applied (Fig. S21†). That is, at these

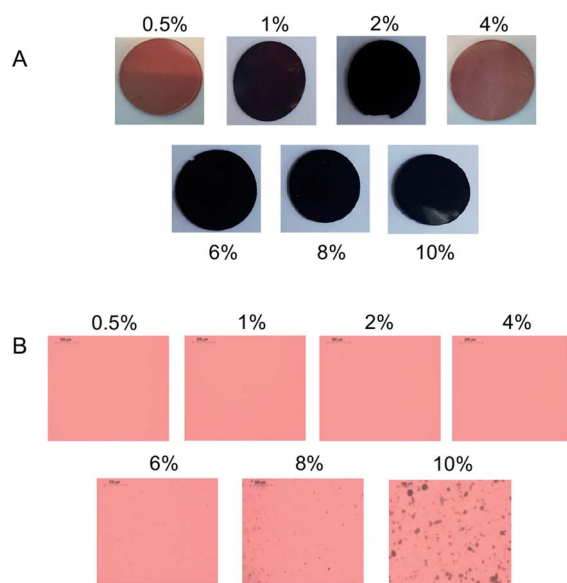
**Fig. 4** (A) Elastomers with increasing weight percentages of Zn-TPMP-Bis-H, 1 mm thick. (B) Optical microscope images of elastomers, 100  $\mu\text{m}$  thick.

Table 4 Summary of dielectric properties and shore OO hardness of elastomers with varying weight percentages of Zn-TPMP-Bis-H elastomers

Weight%, Zn-TPMP-Bis-H	Permittivity @ 0.1 Hz	$\tan \delta$ @ 0.1 Hz	Conductivity @ 0.1 Hz	Shore OO
0	3.08	0.018	$1.16 \times 10^{-13}$	65
0.5	4.15	70.8	$3.48 \times 10^{-11}$	66
1	4.62	98.9	$3.00 \times 10^{-11}$	65
2	5.04	125	$3.54 \times 10^{-11}$	65
4	5.51	194	$4.67 \times 10^{-11}$	63
6	6.75	221	$7.28 \times 10^{-11}$	62
8	7.60	170	$9.36 \times 10^{-11}$	59
10	15.9	150	$1.51 \times 10^{-10}$	59

loadings the phase separated siliconized porphyrin was able to migrate to the air interface, a well-known property of silicone oils,<sup>32</sup> after which point it could easily transfer from the elastomer.

The dielectric behavior of these samples was evaluated. Dielectric permittivity at 0.1 Hz increased with the percentage of Zn-TPMP-Bis-H present in the samples (Table 4). Unlike the Zn-TPMP samples, improvements in the permittivity could be noted even at the lowest loading, 0.5%, which had a permittivity of 4.15, well outside the generally accepted range for unmodified silicone elastomers.<sup>1</sup>

The elastomers all exhibited conductive behavior with a plateau in the conductivity in the region of  $10^{-1}$  to  $10^1$  Hz. Furthermore, in this region the conductivity increased linearly as a function of entrained porphyrin concentration. While the permittivity and conductivity increased in line with loading of Zn-TPMP-Bis-H, changes in the  $\tan \delta$  were not linear; an increase in  $\tan \delta$  was observed as the loading was increased to 6%, but the 8 and 10% samples had lower relative dielectric losses than those of the 4 and 6% samples (Table 4). This changeover in response coincides with the point at which gross phase separation was observed in the sample. Unsurprisingly, then, the  $\tan \delta$  was significantly affected once gross phase separation arose; the relaxation behavior in the two phases is different due to localized conduction in the phases with high concentrations of porphyrin within the elastomer.<sup>33</sup>

### Zn-TPMP-Bis-H at higher loadings

As was the case with the Zn-TPMP system, the Young's moduli of these materials could not be measured due to their relatively poor mechanical properties. Therefore, Shore OO hardness was used to obtain a general idea of the impact of Zn-TPMP-Bis-H on the mechanical properties of the elastomers. Surprisingly, as the loading increased, the Shore OO hardness decreased. The rheological behaviour, specifically the storage moduli of the elastomers exhibited the same trend suggesting that Zn-TPMP-Bis-H has a softening/plasticizing effect on the elastomers (Fig. 5). This outcome is reminiscent of the impact that silicone oils have on elastomers when they are incorporated as an additive; diluting the network with an oil leads to a softer gel.<sup>34</sup> All elastomers, aside from that formed with 10% Zn-TPMP-Bis-H behave like classical, well-crosslinked networks, exhibiting solely high-frequency relaxation. The storage modulus of the

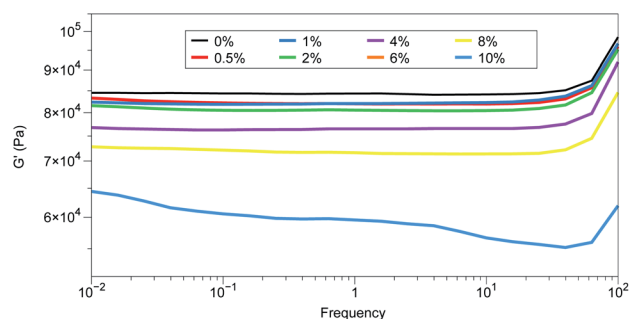


Fig. 5 Storage moduli ( $G'$ ) of Zn-TPMP-Bis-H homemade formulation elastomers @ 25 °C.

10% elastomer shows clear indications of much more complex relaxation behavior. It showed a strong frequency-dependent behavior indicating the emergence and disappearance of transient structures, which may include stacked configurations in the areas with high aromatic content and dangling structures that arise from high content porphyrin phases within the elastomer, which is in agreement with the dielectric properties.

Given the tendency of the self-designed, unfilled model PDMS network to tear, it was deemed to be unsuitable for further testing. Therefore, a more resilient commercial silicone formulation, Elastosil 625, a filled elastomer, was used for all further tests with Zn-TPMP-Bis-H as a dielectric filler.

### Elastosil 625 samples

Elastosil 625 was selected as an alternative for the HMS-301/DMS-V22 system due to its superior mechanical properties, as well as previous performance when used in dielectric applications.<sup>1</sup> Zn-TPMP-Bis-H was dispersed in the two-part Elastosil formulation using the process described above in concentrations of 2, 6 and 10 wt% Zn-TPMP-Bis-H, respectively; these loadings were selected in order to provide a comparison with the homemade system. It was noted that the commercial formulations containing 6 and 10% Zn-TPMP-Bis-H did not cure unless additional catalyst was added (otherwise the product appeared to be a soft gel). To ensure consistency, the same higher catalyst loadings were used with all Elastosil 625 samples containing Zn-TPMP-Bis-H; the amount of additional catalyst added matched the concentration used for the homemade elastomer formulations. IR



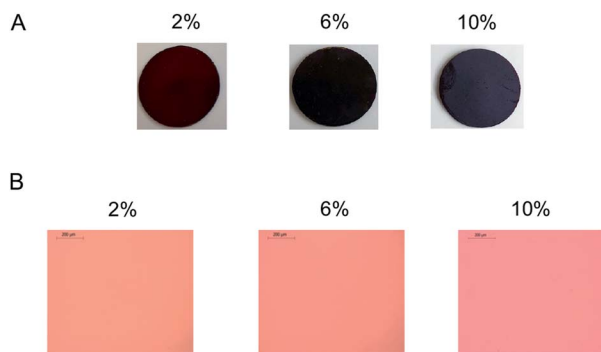


Fig. 6 (A) Elastasil 625 elastomers with increasing weight percentages of Zn-TPMP-Bis-H, 1 mm thick. (B) Optical microscope images of elastomers, 100  $\mu\text{m}$  thick.

spectroscopy was used to confirm complete consumption of Si-H groups (Fig. S20<sup>†</sup>).

The dispersion behaviour of Zn-TPMP-Bis-H in Elastasil 625 was slightly different than in the homemade PDMS system; phase separation at high loadings was not observed (Fig. 6). It is believed that the additives present in Elastasil 625 help to improve the incorporation of Zn-TPMP-Bis-H in the elastomer.<sup>15</sup> However, gross phase separation was still observed in the 10% sample (Fig. S22<sup>†</sup>).

### Young's moduli/rheological properties

Unlike the elastomers made from the homemade PDMS formulation, Elastasil 625 elastomers were not prone to tearing and could be cast as robust thin films. Tensile tests revealed that the Young's moduli decreased as the percentage of porphyrin increased (Table 5). This was surprising, as previous work has shown that increasing the loading of aromatic groups in silicone elastomers results in higher Young's moduli, *via*  $\pi$ - $\pi$  interactions.<sup>35</sup> In this case, it is inferred that the large bis(trimethylsiloxy) group impede aromatic association, such that the porphyrin acts as a plasticizer rather than a reinforcing agent.<sup>34</sup> With Zn-TPMP-Bis-H, the Young's moduli of the elastomers could be reduced even in the presence of the silica reinforcing agents contained within the Elastasil formulation. This is advantageous for dielectric elastomer actuators, as softer materials have better actuation performance.

Table 5 Mechanical properties of Elastasil 625 elastomers

Sample	Young's modulus @ 10% strain (MPa)	Tensile strength (MPa)	Tensile strain (%)
0%	0.65 $\pm$ 0.07	6.22 $\pm$ 2.07	519 $\pm$ 89
2%	0.60 $\pm$ 0.06	3.20 $\pm$ 0.55	418 $\pm$ 33
6%	0.40 $\pm$ 0.05	3.77 $\pm$ 0.62	538 $\pm$ 40
10%	0.16 $\pm$ 0.02	1.96 $\pm$ 0.35	510 $\pm$ 67
10% <sup>a</sup>	0.08 $\pm$ 0.01	1.20 $\pm$ 0.07	435 $\pm$ 19

<sup>a</sup> Sample made with extra Wilkinson's catalyst.

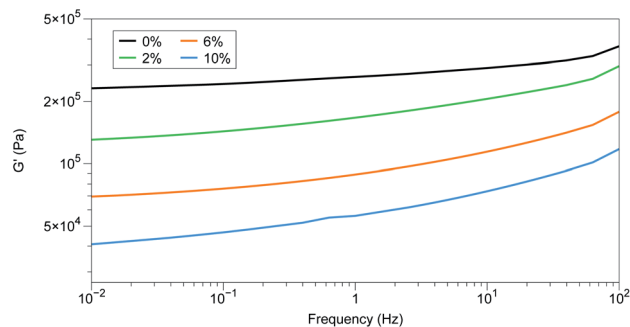


Fig. 7 Storage moduli ( $G'$ ) of Zn-TPMP-Bis-H Elastasil 625 samples @ 25  $^{\circ}\text{C}$ .

Rheological studies of the samples showed that the trend observed in the pure PDMS system – increased loading lowers storage modulus – held for the Elastasil samples as well (Fig. 7). Noticeably absent in the storage moduli results were any characteristics that would indicate phase separation was occurring in the samples, consistent with the lack of phase separation observed in the optical micrographs of the Elastasil elastomers.

### Dielectric properties of Elastasil 625 samples

The dielectric performance of the porphyrin in commercial formulations closely resembled those of the HMS-301+DMS-V22 system; the permittivities increased with increasing Zn-TPMP-Bis-H concentration (Table 6). However, the permittivities in commercial silicone were slightly lower than those measured for the unfilled PDMS samples. The permittivity at the lowest loading level of 2% Zn-TPMP-Bis-H is higher than that usually obtained when using inorganic fillers. For example, elastomers containing  $\text{TiO}_2$ ,  $\text{BaTiO}_2$  or  $\text{ZnO}$  typically require loadings >10% to obtain permittivities greater than 3.<sup>1</sup> The use of inorganic fillers also required specialized mixing techniques where Zn-TPMP-Bis-H can be easily mixed in by hand or, for better consistency, using a speedmixer.

Zn-TPMP-Bis-H also performed favorably when compared to other organic additives; elastomers using only a 10% loading gave permittivities  $\sim$ 13 comparable to those achieved by Zhang *et al.* using CPO, but in the latter case 40% CPO loading was required.<sup>22,23</sup> It compares favorably when compared to other highly conjugated organic systems such poly(hexylthiophene) and polyaniline. In the case of polyaniline, permittivities greater than 8 could not be achieved even at loadings greater than 30%.<sup>20</sup> Poly(hexylthiophene) exhibited very similar permittivity; a loading of 6% poly(hexylthiophene) in silicone had a permittivity of  $\sim$ 14, whereas a 10% loading of Zn-TPMP-Bis-H resulted in a permittivity of  $\sim$ 13.<sup>21</sup>

The Elastasil 625 samples also exhibited a conductive region from  $10^{-1}$ - $10^1$  Hz and, like the homemade system, the conductivity in this region increased with the amount of porphyrin added. The dielectric loss ( $\tan \delta$ ) values @ 0.1 Hz also increased in line with increased loading of porphyrin, reflecting the more homogenous dispersions achieved in the Elastasil samples compared to the initial self-designed elastomers without any additives for *e.g.* improved stability and miscibility.



Table 6 Summary of dielectric properties for Elastosil 625 elastomers in comparison to homemade cure system

Silicone formulation	% Zn-TPMP-Bis-H	Permittivity @ 0.1 Hz	$\tan \delta @ 0.1 \text{ Hz}$	Conductivity @ 0.1 Hz	$F_{OM}$
Homemade	0%	3.08	0.018	$1.16 \times 10^{-13}$	—
	2%	5.04	125	$3.48 \times 10^{-11}$	—
	6%	6.75	221	$7.28 \times 10^{-11}$	—
	10%	15.9	150	$1.51 \times 10^{-10}$	—
Elastosil 625	0%	2.32	0.004	$7.36 \times 10^{-14}$	1.00
	2%	8.67	199	$4.28 \times 10^{-11}$	1.33
	6%	9.68	267	$2.70 \times 10^{-11}$	1.93
	10%	12.7	262	$4.21 \times 10^{-11}$	5.80

To assess the performance of the DEs a figure of merit ( $F_{OM}$ ), described by eqn (2) was calculated, where  $\epsilon'$  is the permittivity of the elastomer,  $\epsilon_0$  is the permittivity in a vacuum,  $E_b$  is the dielectric breakdown strength and  $Y$  is the Young's modulus.<sup>36</sup>

$$F_{om} = \frac{3\epsilon'\epsilon_0 E_b^2}{Y} \quad (2)$$

The  $F_{OM}$  of Elastosil 625 in the absence of additives was calculated and normalized to 1, the results of these calculations are shown in Table 6. From these relative  $F_{OM}$  we can see that the samples containing porphyrin have higher  $F_{OM}$ s than that of the control with the 10% sample having a  $F_{OM}$  6 times greater than that of the control. The increase in the  $F_{OM}$  values is due to the increase in permittivity as well as the reduction in Young's moduli imparted by the porphyrin additive.

### Dielectric breakdown

The dielectric breakdown strength of elastomers was found to have an inverse relationship with the percentage of Zn-TPMP-Bis-H found therein. That is, as the percentage of porphyrin increased the dielectric breakdown strength decreased. This is commonly observed in silicone elastomers when an additive is added; the permittivity increases but the dielectric breakdown strength decreases.<sup>1</sup> However, it is well known that the dielectric breakdown strength of silicone elastomers is affected by the Young's moduli of the materials.<sup>37</sup> In order to ascertain whether the reduction in dielectric breakdown strength is due to a property of the porphyrin or the reduction in Young's modulus, a previously described model (shown in eqn (3)), was applied, where  $E_{BD}$  and  $E_{BD,o}$  refer to the dielectric breakdown strength of the modified and unmodified elastomer (control), respectively,  $k_{BD}^*$  represents the proportionality constant between the Young's modulus and dielectric breakdown strength, and  $Y$  and  $Y_o$  represent the Young's moduli of the modified and unmodified elastomers, respectively.<sup>15</sup>

$$E_{BD} = E_{BD,o} \left( 1 + k_{BD}^* \left( \frac{Y}{Y_o} - 1 \right) \right) \quad (3)$$

A positive  $k_{BD}^*$  value indicates the filler increases the dielectric breakdown strength and that the reduction in dielectric breakdown strength is mainly due the decreased Young's moduli. The calculated  $k_{BD}^*$  values for the porphyrin elastomers

are shown in Table 6 and are positive, suggesting the porphyrin additive serves to increase the dielectric breakdown strength. However, its ability to simultaneously act as a plasticizer, causing decreases in the Young's moduli leads to corresponding reductions in the dielectric breakdown strength despite its role as a voltage stabilizing filler. Further analysis of the dielectric breakdown strengths was conducted using Weibull statistical analysis. Analysis of this data showed that the shape parameter, an indicator of microscopic homogeneity, remained relatively constant for all samples except for the 6% sample that exhibited slightly elevated shape parameter when compared with the other samples (Table 7). This suggests that the 6% sample has the most uniform electrical breakdown, indicating that the sample does consist of a homogenous dispersion of the Zn-TPMP-Bis-H dielectric filler that is also able to act as a voltage stabilizer.<sup>19,33</sup> In other words, the 6% sample exhibits a lower dielectric breakdown strength due to its softness but its electrical properties are enhanced compared to the reference. For large-scale production of dielectric elastomer films the shape parameter is the most crucial parameter, since it as measure of the homogeneity of the materials.<sup>19</sup>

### Actuation tests

The elastomer containing 0% porphyrin was actuated to establish a base line performance for the elastomers. The sample exhibited minimal actuation at low voltages and achieved a maximum area strain of 12% before undergoing dielectric breakdown at  $60 \text{ V } \mu\text{m}^{-1}$ . As expected, the elastomers containing 2, 6 and 10% porphyrin performed better than the control (Fig. 8). Unsurprisingly, given the trend observed in the experimentally measured dielectric breakdown strengths, the 10% sample underwent dielectric breakdown at the lowest

Table 7 Dielectric breakdown strength and Young's modulus for Elastosil 625 samples

Sample	$E_b$ ( $\text{V } \mu\text{m}^{-1}$ )	$\beta$	$\eta$ ( $\text{V } \mu\text{m}^{-1}$ )	$r^2$ of Weibull fit	$Y$ (MPa)	$k_{BD}^*$
0%	$98.4 \pm 4.1$	26.6	100	0.89	$0.65 \pm 0.07$	—
2%	$60.0 \pm 2.4$	27.9	61.0	0.90	$0.60 \pm 0.06$	5.07
6%	$57.3 \pm 2.1$	32.0	58.0	0.94	$0.40 \pm 0.05$	1.08
10%	$50.3 \pm 0.8$	22.0	52.7	0.91	$0.16 \pm 0.02$	0.65



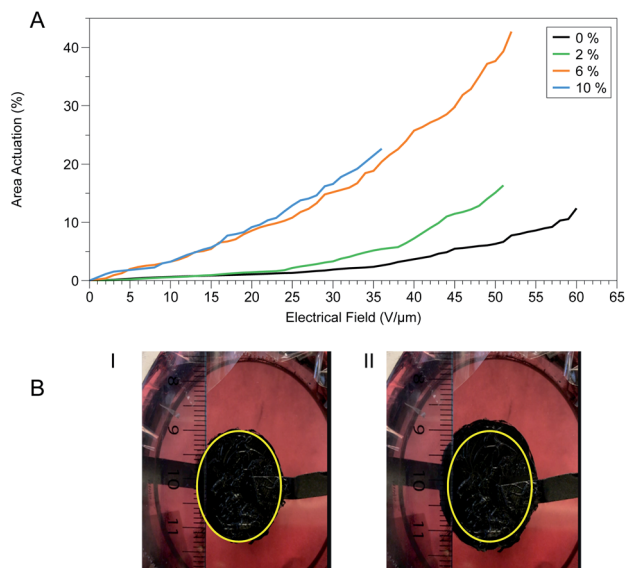


Fig. 8 (A) Actuation performance of 50  $\mu\text{m}$  Elastosil 625 films. (B) (i) 6% elastomer with 0 V applied. (ii) 6% elastomer with 2.55 kV applied (yellow circle indicates unexpanded dimension).

electrical field strength of  $36 \text{ V } \mu\text{m}^{-1}$ , while the 2 and 6% sample exhibited nearly identical breakdown voltages  $51 \text{ V } \mu\text{m}^{-1}$  and  $52 \text{ V } \mu\text{m}^{-1}$ , respectively.

The elastomer with the highest concentration (6%) of well-dispersed Zn-TPMP-Bis-H, confirmed through microscopy and Weibull analysis, exhibited the best performance of the samples tested. Significant actuation, up to  $\sim 8\%$ , could be achieved at voltages below 1 kV and at 1 kV an actuation of  $\sim 10\%$  could be achieved. The 6% sample also continued to actuate as the driving voltage was increased, ultimately achieving a maximum strain of  $\sim 43\%$  before undergoing dielectric breakdown. By comparison, the 2% sample only achieved 1% actuation at 1 kV, the same as the control and the 2% sample was only able to achieve a maximum 12% strain before undergoing dielectric breakdown. The inhomogeneous 10% sample had an almost identical performance to the 6% sample at low voltages, 9% area actuation at 1 kV but, as previously mentioned, suffered from a low dielectric breakdown strength, limiting it to a maximum strain of 22%.

The strains achieved by these materials are an improvement on those achieved by most dielectric elastomer materials; to our knowledge the actuation strains were greater than any inorganic filler previously evaluated.<sup>1</sup> In the case of the most closely related system, which used a 20% loading of organic copper-phthalocyanine oligomers, actuation strains of  $\sim 11\%$  at  $\sim 25 \text{ V } \mu\text{m}^{-1}$  were measured before the sample underwent dielectric breakdown. This compares with the 6% sample tested in this study was able to achieve the same actuation ( $\sim 11\%$ ) at  $25 \text{ V } \mu\text{m}^{-1}$  at a significantly lower loading of additive. Additionally, the siliconized porphyrin was able to continue to actuate at higher field strengths. This can be attributed to the ability to make homogeneous dispersions in the silicone elastomer carrier; that is, the absence of agglomeration contributes to the reduced actuation performance.

When compared to other known organic fillers the Zn-TPMP-Bis-H elastomers also had excellent performance. Elastomers containing poly(hexylthiophene) outperformed the Zn-TPMP-Bis-H elastomers at low fields, as they were able to actuate up to  $\sim 8\%$  at  $6 \text{ V } \mu\text{m}^{-1}$  at a 1% loading vs.  $\sim 3\%$  actuation for 6% Zn-TPMP-Bis-H. However, the use of organic solvents were required to achieve dispersion in the former case. In addition, the samples containing poly(hexylthiophene) were pre-strained by 100% while our samples were only pre-strained by 5%. Finally,  $6 \text{ V } \mu\text{m}^{-1}$  represents the maximum electrical field that can be applied in the case of the poly(hexylthiophene), significantly lower than the maximum field that can be applied to any of the samples used in this study.<sup>21</sup> At  $50 \text{ V } \mu\text{m}^{-1}$  an elastomer containing 15% polyaniline encapsulated in divinylbenzene had an actuation strain of  $\sim 12\%$ , 68% lower than that achieved in the 6% Zn-TPMP-Bis-H sample at the same electrical field.<sup>20</sup>

The actuation performance of the samples evaluated in this study, when compared to literature examples, highlights the promise of macrocycles like porphyrins such as Zn-TPMP-Bis-H as high-permittivity dielectric additives. We are currently examining further modification of the Zn-TPMP core to improve its dispersibility at higher loadings which could lead to even better performing material, eventually allowing for devices that could achieve high strains at low electrical fields removing a potential barrier to commercialization.

## Conclusions

The blending of small quantities, up to 10%, of the modified porphyrin Zn-TPMP-Bis-H served to increase the relative permittivity of silicone elastomers while simultaneously reducing their Young's moduli. Elastomers exhibited homogenous dispersions not previously encountered due to the compatibilization of the porphyrin with silicone elastomers *via* the Piers-Rubinsztajn reaction. Dielectric losses remained low due to the homogeneity of the blends. These factors led to the synthesis of silicone elastomers that could achieve large actuations,  $>40\%$  in response to applied electrical fields in the case of a 6% loading of permittivity-enhancing filler. These elastomers represent a step forward towards the realization of devices that can be commercialized due to their ability to actuate at low electrical fields and at the same time with limited modifications of the commercial elastomers.

## Conflicts of interest

There are no conflicts to declare.

## Acknowledgements

CBG and MAB acknowledge with gratitude financial support from the National Sciences and Research Council of Canada. CBG thanks Mitacs for a Mitacs Globalink Research Award.

## Notes and references

- 1 F. B. Madsen, A. E. Daugaard, S. Hvilsted and A. L. Skov, *Macromol. Rapid Commun.*, 2016, **37**, 378–413.



- 2 R. Pelrine, R. D. Kornbluh, J. Eckerle, P. Jeuck, S. Oh, Q. Pei and S. Stanford, *Dielectric elastomers: generator mode fundamentals and applications*, SPIE, 2001.
- 3 Y. Qiu, E. Zhang, R. Plamthottam and Q. Pei, *Acc. Chem. Res.*, 2019, **52**(2), 316–325.
- 4 L. J. Romasanta, M. A. Lopez-Manchado and R. Verdejo, *Prog. Polym. Sci.*, 2015, **51**, 188–211.
- 5 R. E. Pelrine, R. D. Kornbluh and J. P. Joseph, *Sens. Actuators, A*, 1998, **64**, 77–85.
- 6 D. M. Opris, *Adv. Mater.*, 2018, **30**, 1703678.
- 7 F. Carpi, G. Gallone, F. Galantini and D. De Rossi, in *Dielectric Elastomers as Electromechanical Transducers*, ed. F. Carpi, D. De Rossi, R. Kornbluh, R. Pelrine and P. Sommer-Larsen, Elsevier, Amsterdam, 2008, pp. 51–68.
- 8 G. Gallone, F. Carpi, D. De Rossi, G. Levita and A. Marchetti, *Mater. Sci. Eng., C*, 2007, **27**, 110–116.
- 9 L. Yu and A. L. Skov, *Int. J. Smart Nano Mater.*, 2015, **6**, 268–289.
- 10 H. Zhao, D.-R. Wang, J.-W. Zha, J. Zhao and Z.-M. Dang, *J. Mater. Chem. A*, 2013, **1**, 3140–3145.
- 11 H. Stoyanov, P. Brochu, X. Niu, E. D. Gaspera and Q. Pei, *Appl. Phys. Lett.*, 2012, **100**, 262902.
- 12 L. Yu and A. L. Skov, *RSC Adv.*, 2017, **7**, 45784–45791.
- 13 H. Zhao, L. Zhang, M.-H. Yang, Z.-M. Dang and J. Bai, *Appl. Phys. Lett.*, 2015, **106**, 092904.
- 14 H. Böse, D. Uhl, K. Flittner and H. Schlaak, *Dielectric elastomer actuators with enhanced permittivity and strain*, SPIE, 2011.
- 15 A. L. Skov and L. Yu, *Adv. Eng. Mater.*, 2018, **20**, 1700762.
- 16 H. Zhao, Y.-J. Xia, Z.-M. Dang, J.-W. Zha and G.-H. Hu, *J. Appl. Polym. Sci.*, 2013, **127**, 4440–4445.
- 17 M. Wählander, F. Nilsson, R. L. Andersson, C. C. Sanchez, N. Taylor, A. Carlmark, H. Hillborg and E. Malmström, *J. Mater. Chem. A*, 2017, **5**, 14241–14258.
- 18 L. C. Sim, S. R. Ramanan, H. Ismail, K. N. Seetharamu and T. J. Goh, *Thermochim. Acta*, 2005, **430**, 155–165.
- 19 H. Silau, N. B. Stabell, F. R. Petersen, M. Pham, L. Yu and A. L. Skov, *Adv. Eng. Mater.*, 2018, **20**, 1800241.
- 20 M. Molberg, D. Crespy, P. Rupper, F. Nüesch, J.-A. E. Månson, C. Löwe and D. M. Opris, *Adv. Funct. Mater.*, 2010, **20**, 3280–3291.
- 21 F. Carpi, G. Gallone, F. Galantini and D. De Rossi, *Adv. Funct. Mater.*, 2008, **18**, 235–241.
- 22 C. Löwe, X. Zhang and G. Kovacs, *Adv. Eng. Mater.*, 2005, **7**, 361–367.
- 23 Q. M. Zhang, H. Li, M. Poh, F. Xia, Z. Y. Cheng, H. Xu and C. Huang, *Nature*, 2002, **419**, 284–287.
- 24 E. A. Ough, M. J. Stillman and K. A. M. Creber, *Can. J. Chem.*, 1993, **71**, 1898–1909.
- 25 F. Ghani, J. Kristen and H. Riegler, *J. Chem. Eng. Data*, 2012, **57**, 439–449.
- 26 B. A. Kamino, B. Mills, C. Reali, M. J. Gretton, M. A. Brook and T. P. Bender, *J. Org. Chem.*, 2012, **77**, 1663–1674.
- 27 B. A. Kamino, J. B. Grande, M. A. Brook and T. P. Bender, *Org. Lett.*, 2011, **13**, 154–157.
- 28 M. J. Gretton, B. A. Kamino, M. A. Brook and T. P. Bender, *Macromolecules*, 2012, **45**, 723–728.
- 29 K. M. Smith, D. A. Goff, R. J. Abraham and J. E. Plant, *Org. Magn. Reson.*, 1983, **21**, 505–511.
- 30 F. B. Madsen, I. Dimitrov, A. E. Daugaard, S. Hvilsted and A. L. Skov, *Polym. Chem.*, 2013, **4**, 1700–1707.
- 31 P. Mazurek, S. Vudayagiri and A. L. Skov, *Chem. Soc. Rev.*, 2019, **48**, 1448–1464.
- 32 M. A. Brook, *Silicon in Organic, Organometallic, and Polymer Chemistry*, Wiley, 1999.
- 33 A. H. A. Razak and A. L. Skov, *RSC Adv.*, 2017, **7**, 468–477.
- 34 F. B. Madsen, S. Zakaria, L. Yu and A. L. Skov, *Adv. Eng. Mater.*, 2016, **18**, 1154–1165.
- 35 A. Fatona, J. Moran-Mirabal and M. A. Brook, *Polym. Chem.*, 2019, **10**, 219–227.
- 36 P. Sommer-Larsen and A. L. Larsen, *Materials for dielectric elastomer actuators*, SPIE, 2004.
- 37 L. Yu and A. L. Skov, *Macromol. Rapid Commun.*, 2018, **39**, 1800383.

